ORIGINAL ARTICLE

Hepatology Research

DNA methylation alterations of *ADCY5*, *MICAL2*, and *PLEKHG2* during the developmental stage of cryptogenic hepatocellular carcinoma

Satomi Makiuchi[1] | Ying Tian[1] | Mao Fujimoto[1] | Junko Kuramoto[1] | Noboru Tsuda[1] | Hidenori Ojima[1] | Masahiro Gotoh[2] | Nobuyoshi Hiraoka[3] | Teruhiko Yoshida[2] | Yae Kanai[1] | Eri Arai[1]

[1]Department of Pathology, Keio University School of Medicine, Tokyo, Japan

[2]Fundamental Innovative Oncology Core Center, National Cancer Center Research Institute, Tokyo, Japan

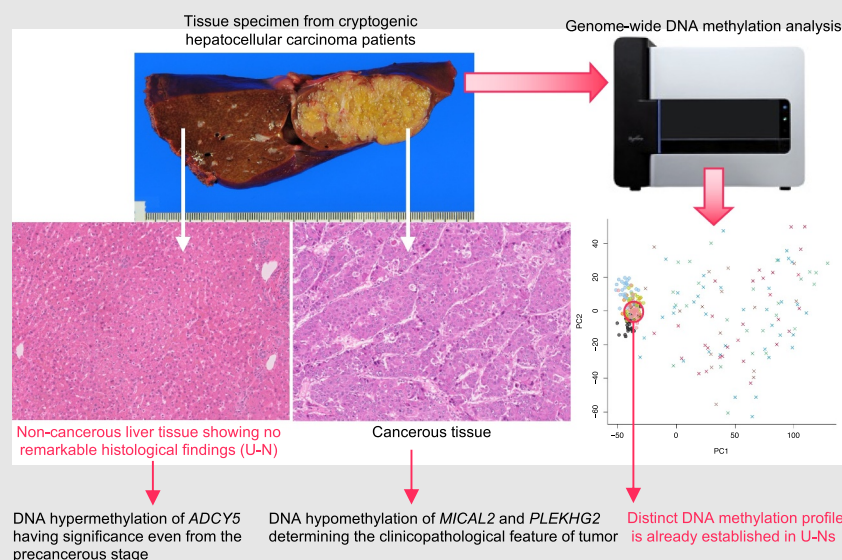[3]Department of Diagnostic Pathology, National Cancer Center Hospital, Tokyo, Japan

Correspondence
Yae Kanai and Eri Arai, Department of Pathology, Keio University School of Medicine, 35 Shinanomachi, Shinjuku-ku, Tokyo 160-8582, Japan.
Email: ykanai@keio.jp and earai@keio.jp

Funding information
Japan Agency for Medical Research and Development

Graphical Abstract

Tissue specimen from cryptogenic hepatocellular carcinoma patients

Genome-wide DNA methylation analysis

Non-cancerous liver tissue showing no remarkable histological findings (U-N)

Cancerous tissue

DNA hypermethylation of *ADCY5* having significance even from the precancerous stage

DNA hypomethylation of *MICAL2* and *PLEKHG2* determining the clinicopathological feature of tumor

Distinct DNA methylation profile is already established in U-Ns

Genome-wide DNA methylation analysis of liver tissue samples has revealed a distinct DNA methylation profile during the developmental stage of cryptogenic hepatocellular carcinoma without a background of nonalcoholic steatohepatitis, viral hepatitis, or alcoholic liver disease. DNA hypermethylation of *ADCY5* resulting in its reduced expression may have significance, even from the precancerous stage, in liver showing no remarkable histological features. DNA hypomethylation of

MICAL2 and *PLEKHG2* in cryptogenic hepatocellular carcinoma may determine the clinicopathological feature of tumors through their overexpression.

Abstract

Aim: The aim of this study was to clarify the significance of DNA methylation alterations of cryptogenic hepatocellular carcinomas (HCCs).

Methods: Using the Infinium assay, we performed genome-wide DNA methylation analysis of 250 liver tissue samples, including noncancerous liver tissue (U-N) and corresponding cancerous tissue (U-T) from patients with cryptogenic HCC without a history of excessive alcohol use and hepatitis virus infection, and whose U-N samples showed no remarkable histological features (no microscopic evidence of simple steatosis, any form of hepatitis including nonalcoholic steatohepatitis, or liver cirrhosis).

Results: We identified 3272 probes that showed significant differences of DNA methylation levels between U-N and normal liver tissue samples from patients without HCC, indicating that a distinct DNA methylation profile had already been established at the precancerous U-N stage. U-Ns have a DNA methylation profile differing from that of noncancerous liver tissue of patients with nonalcoholic steatohepatitis-related, viral hepatitis-related, and alcoholic liver disease-related HCCs. Such DNA methylation alterations in U-Ns were inherited by U-Ts. The U-Ns showed DNA methylation alteration of *ADCY5*, resulting in alteration of its mRNA expression, whereas noncancerous liver tissue of patients with nonalcoholic steatohepatitis-, viral hepatitis-, or alcoholic liver disease-related HCCs did not. DNA methylation levels of *MICAL2* and *PLEKHG2* in U-Ts were correlated with larger tumor diameter and portal vein involvement, respectively.

Conclusions: U-N-specific DNA hypermethylation of *ADCY5* may have significance, even from the precancerous stage in liver showing no remarkable histological features. DNA hypomethylation of *MICAL2* and *PLEKHG2* may determine the clinicopathological features of cryptogenic HCC.

KEYWORDS
ADCY5, cryptogenic hepatocarcinogenesis, genome-wide DNA methylation analysis, hepatocellular carcinoma, *MICAL2*, *PLEKHG2*

INTRODUCTION

DNA methylation is one of the major epigenetic mechanisms, playing an important role in the development of various cancers through chromosomal instability and aberrant expression of tumor-related genes.[1–3] For example, we and other groups have reported that DNA methylation abnormalities are involved in multistage hepatocarcinogenesis related to infection with hepatitis B virus (HBV) or hepatitis C virus (HCV).[4–9] With advances in antihepatitis virus treatment, many studies in recent years have focused on hepatocarcinogenesis in patients with nonalcoholic steatohepatitis (NASH).[10,11]

Our previous genome-wide DNA methylation analysis using the Infinium assay[12] revealed the unique DNA methylation profile of the precancerous NASH stage.[13,14] DNA methylation abnormalities at this stage are inherited by NASH-related hepatocellular carcinomas (HCCs). DNA hypomethylation resulting in increased expression of the *SPHK1* and *LTB* genes in poorly differentiated HCCs may underlie the aggressive phenotype of such HCCs.[15] Moreover, we have identified tumor-related genes, such as *WHSC1*,[13] *TRIM4*, *PRC1*, and *TUBA1B*,[16] whose expression levels are regulated by DNA methylation status, as potential therapeutic targets in NASH-related HCCs.

In contrast, although their incidence is low, HCCs without an etiology of NASH, hepatitis virus infection, or alcohol-induced liver injury can arise even in liver tissue lacking any significant histological changes. Very little is known about the molecular mechanisms underlying the development of such cryptogenic HCCs. We have

observed DNA methylation alterations even in tissue specimens at the precancerous stage showing no remarkable histological features in various organs, such as the kidney[17–19] and urinary bladder.[20–22] These findings suggested that DNA methylation alterations are of significance during carcinogenesis in liver tissue with a normal appearance and lacking any known etiology. In the present study, we attempted to identify DNA methylation profiles in cryptogenic HCCs arising from liver tissue without any significant histological changes. We performed genome-wide DNA methylation analysis of 250 liver tissue specimens, including normal liver tissue, noncancerous and cancerous tissue from patients with cryptogenic HCCs, NASH-related HCCs,[10,11] viral hepatitis-related HCCs,[23] and alcoholic liver disease-related HCCs.[24]

MATERIALS AND METHODS

Patients and tissue samples

For the present analysis, we used 29 paired samples of noncancerous liver tissue (U-N) and corresponding cancerous tissue (U-T) obtained by partial hepatectomy from 29 HCC patients without a history of excessive alcohol use (pure alcohol intake exceeding 30 g/day for men and 20 g/day for women), whose U-N samples showed no remarkable histological features compatible with nonalcoholic fatty liver (i.e., simple steatosis); any form of hepatitis, including steatohepatitis satisfying the criteria for NASH;[25] any form of liver cirrhosis; or autoimmune liver disease. All 29 patients were negative for both HBV surface antigen and anti-HCV antibody. Therefore, we considered the 29 U-T samples to be cryptogenic HCCs.

For comparison, we also examined 25 paired samples of noncancerous liver tissue (NASH-N) and corresponding cancerous tissue (NASH-T) obtained by partial hepatectomy from 25 NASH patients, 37 paired samples of noncancerous liver tissue (V-N) and corresponding cancerous tissue (V-T) obtained by partial hepatectomy from 37 patients positive for HBV ($n = 15$), HCV ($n = 21$) or both ($n = 1$) with chronic hepatitis or liver cirrhosis, and 16 paired samples of noncancerous liver tissue (AL-N) and corresponding cancerous tissue (AL-T) obtained by partial hepatectomy from 16 patients with alcoholic liver disease. HCCs were diagnosed histologically in accordance with the World Health Organization classification.[26] Representative histological features of U-N, U-T, NASH-N, NASH-T, V-N, and V-T are shown in Figure 1. As shown in Figure 1a, hematoxylin–eosin staining showed an absence of inflammatory cells in both the portal area and intralobular region in U-N samples. This was confirmed by immunohistochemistry using antibodies against CD3, CD20, and CD68; that is, markers for T cells, B cells, and macrophages, respectively (Figure S1). In V-N and NASH-N, numerous T cells, many B cells, and a few macrophages had infiltrated into the portal area, and intralobular infiltration of T and B cells, and macrophages was observed, whereas U-N was devoid of any T- and B-cell or macrophage infiltration, although tissue-resident macrophages were

observed even in U-N (Figure S1). The clinicopathological parameters of all 107 HCC patients with U-T, NASH-T, V-T, or AL-T are summarized in Table S1.

In addition, 36 samples of normal control liver tissue (NLT) showing no remarkable histological features obtained by partial hepatectomy from HBV-negative and HCV-negative patients with liver metastasis of primary colorectal cancer, but without a history of excessive alcohol use, chronic hepatitis, liver cirrhosis, nonalcoholic fatty liver disease (nonalcoholic fatty liver and NASH), or HCC, were examined. Therefore, as categorized in Table S2, a total of 250 liver tissue samples were included in the present study.

All 143 patients with HCC or liver metastasis of primary colorectal cancer underwent partial hepatectomy at the National Cancer Center Hospital, Tokyo, Japan; none of the patients had received preoperative anticancer treatment. Immediately after surgical removal, all tissue specimens were frozen in liquid nitrogen and stored until use in research in accordance with the Japanese Society of Pathology Guidelines for the handling of pathological tissue samples for genomic research.[27]

Infinium assay

Genome-wide DNA methylation analysis was performed using the Infinium HumanMethylation450 BeadChip (Illumina, San Diego, CA, USA). Details are described in Supplementary Methods. Infinium data for 25 NASH-Ns, 25 NASH-Ts, 37 V-Ns, 37 V-Ts, and 36 NLTs were also included in our previous papers focusing on NASH-related hepatocarcinogenesis: 29 U-Ns, 29 U-Ts, 16 AL-Ns, and 16 AL-Ts (90 samples in total) were originally examined for this study.[13–16]

Real-time quantitative reverse transcription polymerase chain reaction analysis

Levels of expression of mRNA for the *ADCY5*, *MICAL2*, and *PLEKHG2* genes were determined by reverse transcription polymerase chain reaction (RT–PCR) analysis using the primer sets summarized in Table S3. Details are described in Supplementary Methods.

5-Aza-2′-deoxycytidine treatment of cell lines

The human HCC cell lines, PLC/PRF/5,[28] JHH-7,[29] and HepG2[30] were purchased from the Japanese Collection of Research Bioresources (Osaka, Japan). Although liver tissue contains both parenchymal and nonparenchymal cells, as shown in Figures 1a and 1b, U-N and U-T specimens consisted primarily of hepatocytes and hepatocellular carcinoma cells, respectively, and contained fewer nonparenchymal cells. For this reason, we decided to use HCC cell lines for experiments using 5-aza-2′-deoxycytidine (5-aza-dC). Details are described in Supplementary Methods.
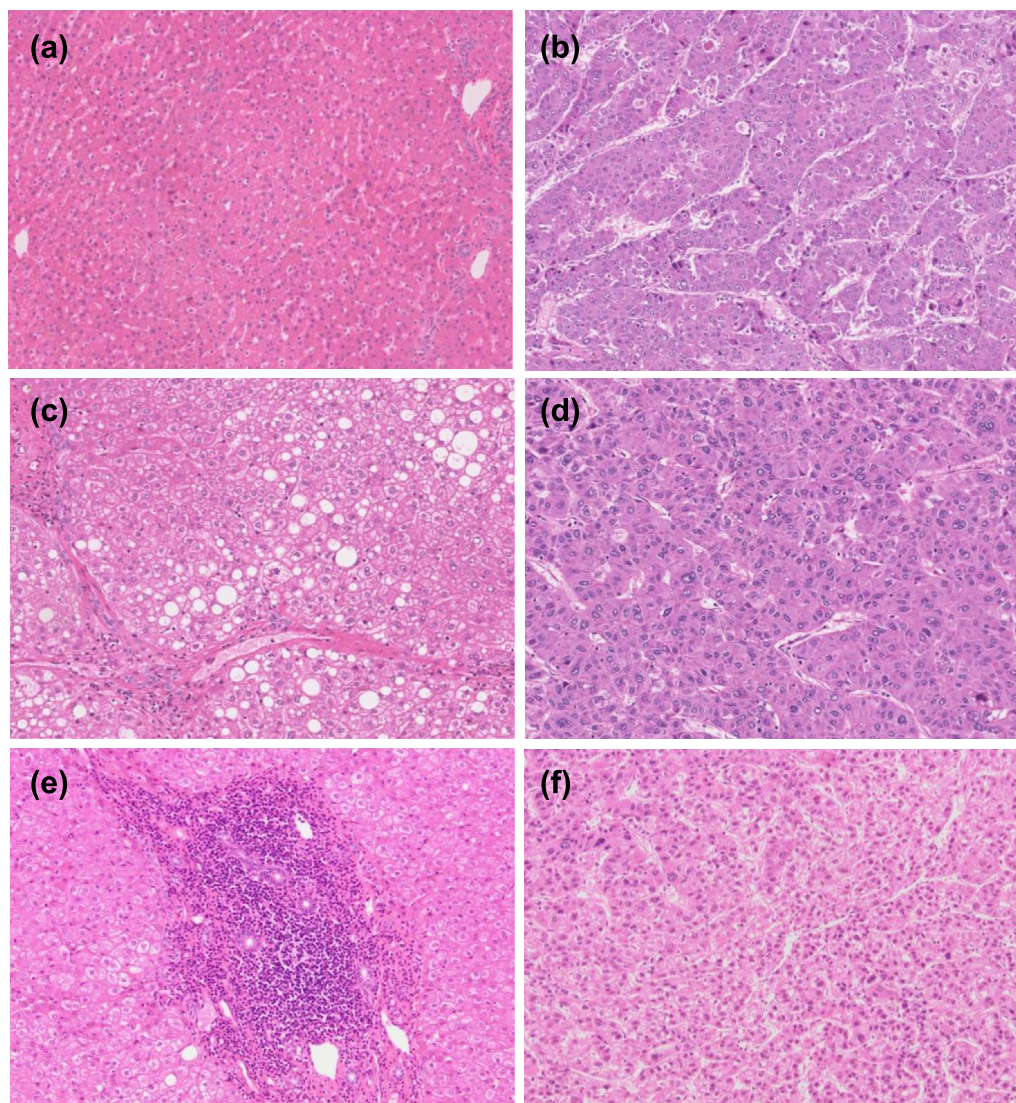
FIGURE 1 (a, c, e) Representative photos of noncarcinomatous liver tissue and (b, d, f) the corresponding hepatocellular carcinoma (HCC) from patients with (a, b) cryptogenic HCC without a background of nonalcoholic steatohepatitis, viral hepatitis or alcoholic liver disease, (c, d) nonalcoholic steatohepatitis -related HCC, and (e, f) viral hepatitis-related HCC. Hematoxylin–eosin staining. Original magnification: ×10.

Statistical analysis

In the Infinium assay, the call proportions (p-value < 0.01 for detection of signals above the background) for 729 probes in all 250 tissue samples were less than 90%. Because such a low proportion may have been attributable to polymorphism at the probe CpG sites, these 729 probes were excluded from the present assay, as described previously.[31,32] In addition, 620 probes containing missing β-values of more than 10% were excluded. Finally, to avoid any sex-specific methylation bias, all 11 648 probes on chromosomes X and Y were also excluded, leaving a final total of 470 356 autosomal CpG sites.

The DNA methylation profile was analyzed using principal component analysis and hierarchical clustering (complete linkage method using Euclidean distance). Significant differences in DNA methylation and mRNA expression levels between sample groups were defined by Welch's t-test and the Jonckheere–Terpstra trend test adjusted by Bonferroni correction. Correlations between epigenomic clusters and clinicopathological parameters were examined using Fisher's exact test and the Kruskal–Wallis test. Correlations between the methylation levels of CpG sites located within the CpG island, N-Shelf (2000-bp region 5′ adjacent to N-Shore), N-Shore (2000-bp region 5′ adjacent to CpG island), S-Shore (2000-bp region 3′ adjacent to CpG island), and S-Shelf (2000-bp region 3′ adjacent to S-Shore) based on the University of California, Santa Cruz Genome Browser (https://genome.ucsc.edu/) and annotated around the transcription start sites (TSSs) of any genes, such as the region from 200 bp upstream of the TSS to 1500 bp upstream of it (TSS1500), the region from TSS to 200 bp upstream of TSS (TSS200), the 5′ untranslated region, the first exon or the first intron, and mRNA expression levels of the annotated genes were examined by Pearson's correlation coefficient ($r < -0.2$, $p < 0.05$) using The Cancer Genome Atlas database (https://cancergenome.nih.gov). Pathway analysis was performed by

the Reactome database (https://reactome.org). All statistical analyses were performed using the programing language R (The R Foundation for Statistical Computing, Vienna, Austria).

RESULTS

DNA methylation alterations during cryptogenic hepatocarcinogenesis

To gain an overview of the DNA methylation profiles of all 250 liver tissue samples, principal component analysis was performed using the DNA methylation levels of all 470 356 probes (Figure 2). DNA methylation profiles of all HCC samples (U-T, NASH-T, V-T, and AL-T) were different from those of both NLT samples and noncancerous liver tissue samples (U-N, NASH-N, V-N, and AL-N; Figure 2), indicating that DNA methylation alterations are associated with hepatocarcinogenesis irrespective of the presence or absence of chronic liver diseases.

Samples of noncancerous liver tissue from patients with HCCs (NASH-N, V-N, and AL-N) showed distinct DNA methylation profiles differing from those of NLTs. Even though U-N samples showed no remarkab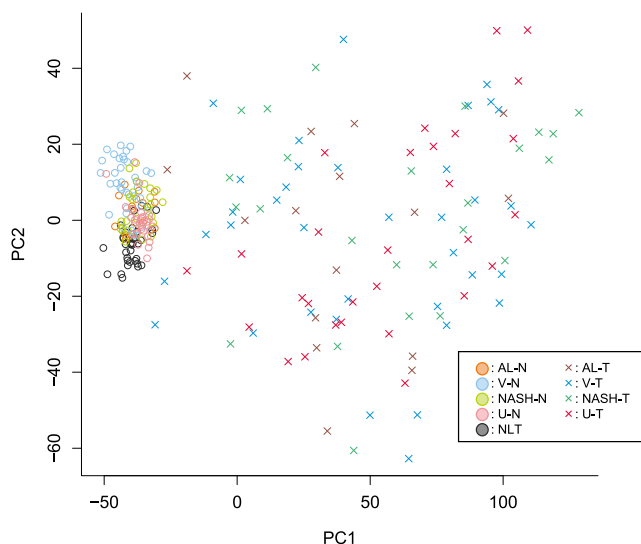le histological features as NLT samples, the DNA methylation profiles of U-Ns differed from those of NLT (Figure 2). We identified 3272 probes that showed significant differences of DNA methylation levels between 29 U-N samples and 36 NLT samples (Welch's t-test adjusted by Bonferroni correction, $p < 0.05$). Among these 3272 probes, 622 and 2650 showed DNA hyper- ($\beta_{U-N} > \beta_{NLT}$) and hypo-($\beta_{U-N} < \beta_{NLT}$) methylation in U-N samples relative to NLT samples, respectively. No significant differences in history and laboratory data relating to diabetes mellitus, hyperlipidemia, hypertension, and smoking were observed between the two cohorts from whom NLT and U-N samples were obtained (Table S4). Therefore, differences in DNA methylation profiles between NLT samples and U-N samples were not attributable to differences in underlying systemic condition.

Among the 3272 probes, 2454 probes showed ordered differences in DNA methylation levels from NLT samples to U-N samples and then to U-T samples (Jonckheere–Terpstra trend test adjusted by Bonferroni correction, $p < 0.05$). On representative probes from the 2454, ordered differences in DNA methylation status are shown in Figure 3. DNA hypermethylation at the precancerous U-N stages was inherited by or strengthened in U-T samples themselves for 387 probes (Figure 3a), whereas DNA hypomethylation at the precancerous U-N stages was inherited by or strengthened in U-T samples for the remaining 2067 probes (Figure 3b).

Epigenetic clustering of patients with HCCs based on the DNA methylation profiles of their noncancerous liver tissue samples

Hierarchical clustering (complete linkage method using Euclidean distance) was performed for noncancerous liver tissues (U-N, NASH-N, V-N, and AL-N) from 107 patients using DNA methylation levels at all 470 356 probes (β_{U-N}, β_{NASH-N}, β_{V-N}, and β_{AL-N}). The HCC patients were subclustered into clusters I ($n = 22$), II ($n = 27$), III ($n = 38$), and IV ($n = 20$; Figure 4). The clinicopathological parameters of the patients in each cluster are summarized in Table 1.

The majority of patients (23 patients of 29) with cryptogenic HCCs were included in cluster III ($p = 5.00 \times 10^{-4}$; Table 1); such patients were significantly more frequent in cluster III (60%) than in clusters I, II, and IV (8.7%, $p = 3.76 \times 10^{-5}$; Figure 4). In contrast, all of the patients in cluster I suffered from viral hepatitis-related HCC, whereas NASH-related HCC patients accounted for the largest population of cluster II (Figure 4).

Furthermore, patients belonging to cluster III were older than patients belonging to cluster I ($p = 2.73 \times 10^{-3}$; Table 1); this characteristic of cluster III was consistent with that of patients with U-T, who showed a significantly higher average age ($p = 4.75 \times 10^{-3}$) than patients with NASH-T, V-T, and AL-T (Table S5). Even though the epigenomic clustering was based on DNA methylation profiles of noncancerous liver tissue, HCCs of patients belonging to cluster III more frequently showed a larger diameter ($p = 4.15 \times 10^{-4}$) and hepatic vein involvement ($p = 9.11 \times 10^{-3}$; Table 1). Such characteristics of cluster III were consistent with those of U-Ts, themselves showing a significantly larger diameter ($p = 2.28 \times 10^{-4}$) than NASH-T, V-T, and AL-T (Table S5).

FIGURE 2 Principal component analysis of normal liver tissue (NLT) from patients with liver metastasis of primary colorectal cancer without a history of excessive alcohol use, chronic hepatitis, liver cirrhosis or hepatocellular carcinoma (HCC; $n = 36$), noncancerous liver tissue from patients with cryptogenic HCC without a background of NASH, viral hepatitis or alcoholic liver disease (U-N; $n = 29$), noncancerous liver tissue from patients with NASH-related HCC (NASH-N; $n = 25$), noncancerous liver tissue from patients with viral hepatitis-related HCC (V-N; $n = 37$), noncancerous liver tissue from patients with alcoholic liver disease-related HCC (AL-N; $n = 16$), cryptogenic HCC (U-T; $n = 29$), NASH-related HCC (NASH-T; $n = 25$), viral hepatitis-related HCC (V-T; $n = 37$), and alcoholic liver disease-related HCC (AL-T; $n = 16$) using the DNA methylation levels of all 470 356 probes. PC, principal component.

FIGURE 3 Ordered differences in DNA methylation levels for representative probes (Jonckheere–Terpstra trend test, adjusted Bonferroni correction; $p < 0.05$), which were aberrantly methylated even in noncancerous liver tissue from patients with cryptogenic hepatocellular carcinoma without a background of nonalcoholic steatohepatitis, viral hepatitis or alcoholic liver disease (U-N; $n = 29$) compared with normal liver tissues (NLT; $n = 36$). Infinium probe IDs and gene names are shown at the top of each panel. (a) DNA hypermethylation at the precancerous U-N stages relative to NLT samples was inherited by or strengthened in cryptogenic hepatocellular carcinoma (U-T) samples themselves ($n = 29$). (b) DNA hypomethylation at the precancerous U-N stages relative to NLT samples was strengthened in U-T samples themselves.
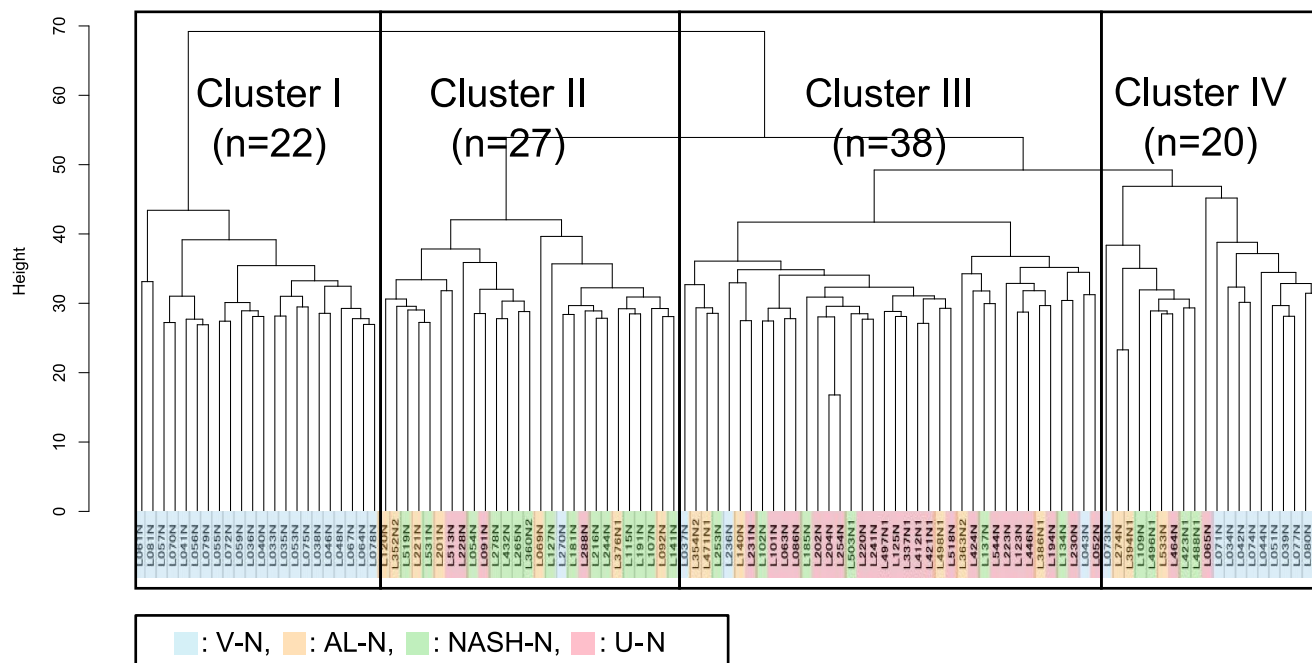
FIGURE 4 Unsupervised hierarchical clustering (Euclidean distance, complete linkage method) in noncancerous liver tissue from patients with cryptogenic hepatocellular carcinoma (HCC; U-N; $n = 29$), noncancerous liver tissue from patients with nonalcoholic steatohepatitis (NASH)-related HCC (NASH-N; $n = 25$), noncancerous liver tissue from patients with viral hepatitis-related HCC (V-N; $n = 37$), noncancerous liver tissue from patients with alcoholic liver disease-related HCC (AL-N; $n = 16$) using DNA methylation levels for all 470 356 probes ($\beta_{U-N}$, β_{NASH-N}, β_{V-N}, and β_{AL-N}). The HCC patients were subclustered into clusters I ($n = 22$), II ($n = 27$), III ($n = 38$), and IV ($n = 20$) based on the DNA methylation profiles of their noncancerous liver tissue samples.

Differences of DNA methylation profiles between cryptogenic hepatocarcinogenesis and NASH-, viral hepatitis-, and alcoholic liver disease-related hepatocarcinogenesis

A small number of U-N samples were found in clusters other than cluster III; that is, NASH-N-dominated cluster II and V-N-dominated cluster IV. U-N samples in clusters II and IV might have been from patients with some degree of fatty liver disease or with previous hepatitis virus infection, respectively, which had been clinically underestimated and did not result in any remarkable histological changes to the liver when examined microscopically. Therefore, U-N samples in clusters II and IV may have been on carcinogenetic pathways similar to those involved in the development of NASH-T and V-T, respectively. In subsequent analyses, we then focused on the differences between U-N samples belonging to cluster III (23 samples in total, termed "U_{III}-N" hereafter), and noncancerous liver tissue samples with other types of etiology grouped into clusters I, II, and IV; that is, 19 NASH-N samples, 34 V-N samples, and 10 AL-N samples (63 samples in total, termed "Other$_{I, II, IV}$-N" hereafter).

To clarify the DNA methylation profiles of U_{III}-N, we identified 9200 probes that showed significant differences in DNA methylation levels between U_{III}-Ns and Other$_{I, II, IV}$-Ns (Welch's t-test adjusted by Bonferroni correction, $p < 0.05$, and a $\Delta\beta_{UIII-N - OtherI, II, IV-N}$ value of more than 0.1 or less than −0.1). Among the 9200 probes, 2189 were located within the CpG island, N-Shelf, N-Shore, S-Shore, and S-Shelf,

and annotated around the TSSs of any genes, such as TSS1500, TSS200, the 5′ untranslated region, the first exon or the first intron. Of the 2189 probes, 906 were annotated to 616 genes showing a significant inverse correlation between the levels of DNA methylation and mRNA expression ($r < −0.2$, $p < 0.05$) using data for 308 samples of cancerous and noncancerous liver tissue deposited in The Cancer Genome Atlas database. These 906 probes are summarized in Table S6.

Reactome pathway analysis showed that the 616 genes in Table S6, whose DNA methylation levels differed between U_{III}-N and Other$_{I, II, IV}$-N, and potentially regulated their mRNA expression levels, were significantly (FDR<0.25) accumulated in 17 signaling pathways (Table S7). Most of these 17 pathways are involved in the metabolism of biological substances, such as "metabolism of vitamins and cofactors" ($p = 5.73 \times 10^{-6}$, FDR $= 2.75 \times 10^{-3}$) and "metabolic abnormalities and diseases" ($p = 8.05 \times 10^{-4}$, FDR $= 1.00 \times 10^{-1}$; Table S7).

Identification of a gene showing DNA methylation alteration specific to cryptogenic hepatocarcinogenesis even from the precancerous stage

Among the 616 genes, 10 showed significant differences of DNA methylation levels even between U_{III}-N samples ($n = 23$) and NLT

TABLE 1 Correlations between epigenetic clustering based on DNA methylation profiles in noncancerous liver tissue samples and clinicopathological parameters of patients with hepatocellular carcinoma.

Clinicopathological parameters	Cluster I ($n = 22$)	Cluster II ($n = 27$)	Cluster III ($n = 38$)	Cluster IV ($n = 20$)	p^a
Patients					
Etiology					
Cryptogenic HCC	0 (0%)	4 (14.8%)	23 (60.5%)	2 (10%)	5.00×10^{-4b}
NASH	0 (0%)	15 (55.6%)	6 (15.8%)	4 (20%)	
Viral hepatitis	22 (100%)	1 (3.7%)	3 (7.9%)	11 (55%)	
Alcoholic liver disease	0 (0%)	7 (25.9%)	6 (15.8%)	3 (15%)	
Age (years)					
Median	61	70	71	68	2.73×10^{-3c}
Interquartile range	56–66	65–75	67–74	60–73	
Sex					
Male	19 (86.4%)	25 (92.6%)	32 (84.2%)	17 (85%)	7.90×10^{-1b}
Female	3 (13.6%)	2 (7.4%)	6 (15.8%)	3 (15%)	
Hepatocellular carcinoma					
Largest diameter (mm)					
<50	19 (86.4%)	16 (59.3%)	12 (31.6%)	10 (50%)	4.15×10^{-4b}
≥50	3 (13.6%)	11 (40.7%)	26 (68.4%)	10 (50%)	
Differentiation					
Well	5 (22.7%)	7 (25.9%)	5 (13.2%)	4 (20%)	3.38×10^{-1b}
Moderately	8 (36.4%)	16 (59.3%)	24 (63.2%)	11 (55%)	
Poorly	9 (40.9%)	4 (14.8%)	9 (23.7%)	5 (25%)	
Portal vein involvement					
Negative	10 (45.5%)	14 (51.9%)	10 (26.3%)	8 (40%)	1.79×10^{-1b}
Positive	12 (54.5%)	13 (48.1%)	28 (73.7%)	12 (60%)	
Hepatic vein involvement					
Negative	22 (100%)	25 (92.6%)	27 (71.1%)	17 (85%)	9.11×10^{-3b}
Positive	0 (0%)	2 (7.4%)	11 (28.9%)	3 (15%)	
Bile duct invasion					
Negative	22 (100%)	25 (92.6%)	36 (94.7%)	20 (100%)	5.90×10^{-1b}
Positive	0 (0%)	2 (7.4%)	2 (5.3%)	0 (0%)	
Intrahepatic metastasis					
No	14 (63.6%)	22 (81.5%)	32 (84.2%)	16 (80%)	3.08×10^{-1b}
Yes	8 (36.4%)	5 (18.5%)	6 (15.8%)	4 (20%)	

[a]p-values of <0.05 are underlined.
[b]Fisher's exact test.
[c]Kruskal–Wallis test.

samples ($n = 36$; $p < 0.05$ after Bonferroni correction; Table 2). Among the 10 genes, nine showed significant differences of DNA methylation levels even between Other$_{I, II, IV}$-N samples ($n = 63$) and NLT samples ($n = 36$), leaving only one gene, *ADCY5*, showing U$_{III}$-N-specific DNA methylation alterations (Table 2). A flowchart explaining the steps used to extract *ADCY5* is shown as Figure S2.

Identification of genes potentially affecting the clinicopathological features of cryptogenic HCCs through DNA methylation abnormalities

Correlations between clinicopathological parameters and DNA methylation levels of the 906 probes (Table S6) in U-T samples

TABLE 2 Identification of a gene showing DNA methylation alterations specific to noncancerous liver tissue from patients with cryptogenic hepatocellular carcinoma without a background of nonalcoholic steatohepatitis, viral hepatitis, or alcoholic liver disease belonging to cluster III.

Gene symbol	Probe ID[a]	CpG type[b]	Annotation[c]	Normal liver tissue samples ($n = 36$) DNA methylation levels (mean ± SD)	U_{III}-N samples ($n = 23$) DNA methylation levels (mean ± SD)	$p^{[d]}$ for Other$_{I, II, IV}$-N	$p^{[d]}$ for NLT	Noncancerous liver tissue samples from patients with NASH-, viral hepatitis-, or alcoholic liver disease-related HCC belonging to clusters I, II, and IV (Other$_{I, II, IV}$-N; $n = 63$) DNA methylation levels (mean ± SD)	$p^{[d]}$ for NLT
ADCY5	cg04908625	Island	1st exon	0.518 ± 0.055	0.653 ± 0.044	$\underline{1.38 \times 10^{-3}}$	$\underline{5.78 \times 10^{-9}}$	0.552 ± 0.095	1
CYBA	cg05744675	N_Shelf; S_Shore	TSS1500	0.564 ± 0.056	0.450 ± 0.051	$\underline{1.27 \times 10^{-3}}$	$\underline{7.24 \times 10^{-5}}$	0.329 ± 0.115	$\underline{3.36 \times 10^{-18}}$
RAB3D	cg05896042	Island	5′UTR/1st intron	0.609 ± 0.058	0.487 ± 0.059	$\underline{1.33 \times 10^{-3}}$	$\underline{2.86 \times 10^{-4}}$	0.341 ± 0.145	$\underline{1.52 \times 10^{-16}}$
RCN3	cg19403104	S_Shelf; Island	5′UTR/1st exon	0.591 ± 0.035	0.541 ± 0.021	$\underline{1.88 \times 10^{-9}}$	$\underline{2.26 \times 10^{-3}}$	0.414 ± 0.097	$\underline{1.57 \times 10^{-16}}$
ZNF385A	cg07000334	S_Shore	TSS200	0.658 ± 0.052	0.582 ± 0.039	$\underline{2.33 \times 10^{-7}}$	$\underline{1.18 \times 10^{-2}}$	0.470 ± 0.080	$\underline{1.47 \times 10^{-19}}$
KCNQ4	cg13438961	Island	1st exon	0.592 ± 0.057	0.495 ± 0.054	$\underline{2.85 \times 10^{-7}}$	$\underline{1.33 \times 10^{-2}}$	0.339 ± 0.112	$\underline{4.86 \times 10^{-21}}$
ELFN1	cg08410691	S_Shore	5′UTR/1st intron	0.282 ± 0.047	0.350 ± 0.035	$\underline{1.14 \times 10^{-6}}$	$\underline{3.17 \times 10^{-2}}$	0.455 ± 0.082	$\underline{1.09 \times 10^{-17}}$
ARHGEF2	cg00246451	S_Shore	5′UTR/1st exon	0.671 ± 0.055	0.598 ± 0.035	$\underline{1.34 \times 10^{-9}}$	$\underline{3.60 \times 10^{-2}}$	0.467 ± 0.092	$\underline{5.48 \times 10^{-19}}$
ARHGEF2	cg00246451	S_Shore	TSS1500	0.671 ± 0.055	0.598 ± 0.035	$\underline{1.34 \times 10^{-9}}$	$\underline{3.60 \times 10^{-2}}$	0.467 ± 0.092	$\underline{5.48 \times 10^{-19}}$
HADH	cg27527503	N_Shore	TSS1500	0.396 ± 0.059	0.490 ± 0.054	$\underline{4.09 \times 10^{-5}}$	$\underline{4.05 \times 10^{-2}}$	0.620 ± 0.101	$\underline{4.12 \times 10^{-19}}$

[a]Probe ID of the Infinium HumanMethylation 450 BeadChip.

[b]N_Shelf: 2000 bp region 5′ adjacent to N_Shore; N_Shore: 2000 bp region 5′ adjacent to CpG island; S_Shore: 2000 bp region 3′ adjacent to CpG island; S_Shelf: 2000 bp region 3′ adjacent to S_Shore.

[c]Probe CpG sites were annotated as the region from 200 bp upstream of the transcription start site (TSS) to 1500 bp upstream of it (TSS1500), the region from TSS to 200 bp upstream of TSS (TSS200), the 5′ untranslated region (5′UTR), the first exon and the first intron.

[d]p-values (Welch's t-test, adjusted by Bonferroni correction) <0.05 are underlined.

belonging to cluster III (U_{III}-T samples) were examined. The 124 probes designed for 104 genes showed significant correlations between DNA methylation levels in U_{III}-T samples and the largest tumor diameter or portal vein involvement (Table S8). Among the 104 genes, the top 10 genes showing the lowest p-values for largest diameter and portal vein involvement are summarized in Table 3. Correlations with clinicopathological parameters for MICAL2 and PLEKHG2, the top genes for the largest diameter and portal vein involvement, respectively, were U_{III}-T-specific; such correlations for MICAL2 and PLEKHG2 were not observed in Other$_{I, II, IV}$-T samples.

mRNA expressions of cryptogenic HCC-related genes in tissue specimens

mRNA expression of ADCY5 was significantly reduced in U_{III}-N samples relative to NLT samples ($p = 3.41 \times 10^{-2}$ by Welch's t test), and then further reduced in U_{III}-T samples ($p = 2.16 \times 10^{-6}$ by Welch's t-test and $p = 1.00 \times 10^{-9}$ by Jonckheere–Terpstra trend test), along with the ordered DNA hypermethylation in U_{III}-N samples relative to NLT samples ($p = 7.59 \times 10^{-14}$ by Welch's t-test), and then further in U_{III}-T samples ($p = 1.11 \times 10^{-8}$ by Welch's t-test and $p < 2.20 \times 10^{-16}$ by Jonckheere–Terpstra trend test; Figure 5a). In contrast, expression of ADCY5 mRNA was decreased even in Other$_{I,II,IV}$-N samples relative to NLT samples, and further decreased in Other$_{I,II,IV}$-T samples (Figure S3), indicating that mechanisms other than DNA hypermethylation participate in the reduced expression of ADCY5 even in the developmental stage of Other$_{I, II, IV}$-T.

mRNA expression of MICAL2 showed a tendency to be elevated in U_{III}-T samples with a diameter of 5 cm or more relative to U_{III}-T samples with a diameter of less than 5 cm, along with DNA hypomethylation in U_{III}-T samples with a diameter of 5 cm or more ($p = 1.21 \times 10^{-7}$ by Welch's t-test; Figure 5b).

TABLE 3 Correlations between DNA methylation levels in cancerous tissue of patients with cryptogenic hepatocellular carcinoma belonging to cluster III and clinicopathological parameters.

Gene symbol	Probe ID[a]	Largest tumor diameter (mm)		$\|\Delta\beta\|$[b]	p
		<50 ($n = 4$, mean ± SD)	≥50 ($n = 19$, mean ± SD)		
Top 10 genes showing significant differences of DNA methylation levels between HCCs <50 mm in diameter and those measuring ≥50 mm					
MICAL2	cg12122057	0.698 ± 0.029	0.431 ± 0.134	0.266	1.25×10^{-7}
MIB2	cg10970349	0.841 ± 0.017	0.547 ± 0.214	0.294	1.11×10^{-5}
NAPEPLD	cg03532673	0.328 ± 0.026	0.200 ± 0.079	0.128	2.71×10^{-5}
TOLLIP	cg17152436	0.923 ± 0.068	0.613 ± 0.259	0.311	2.17×10^{-4}
OTUB1	cg20687940	0.116 ± 0.049	0.401 ± 0.266	0.285	2.97×10^{-4}
TOLLIP	cg12089204	0.875 ± 0.034	0.718 ± 0.139	0.157	3.28×10^{-4}
WDR81	cg07085177	0.811 ± 0.032	0.657 ± 0.143	0.154	4.03×10^{-4}
MICAL2	cg24022152	0.750 ± 0.065	0.519 ± 0.185	0.230	6.22×10^{-4}
GPR39	cg07785936	0.368 ± 0.018	0.301 ± 0.068	0.067	1.45×10^{-3}
PRXL2A	cg07091481	0.409 ± 0.040	0.289 ± 0.100	0.120	1.84×10^{-3}
Gene symbol	Probe ID[a]	Portal vein involvement		$\|\Delta\beta\|$[b]	p
		Negative ($n = 7$, mean ± SD)	Positive ($n = 16$, mean ± SD)		
Top 10 genes showing significant differences of DNA methylation levels between HCCs with portal vein involvement and those without it					
PLEKHG2	cg18302606	0.757 ± 0.057	0.514 ± 0.300	0.244	6.04×10^{-3}
PLEC	cg14324585	0.532 ± 0.146	0.306 ± 0.173	0.227	6.27×10^{-3}
MTCH2	cg07304015	0.238 ± 0.064	0.389 ± 0.177	0.150	7.17×10^{-3}
BHMT2	cg06787519	0.320 ± 0.085	0.477 ± 0.175	0.158	8.61×10^{-3}
ABHD18	cg03385262	0.815 ± 0.076	0.643 ± 0.217	0.172	1.06×10^{-2}
CABYR	cg25364343	0.677 ± 0.168	0.398 ± 0.311	0.279	1.15×10^{-2}
BHMT2	cg17213304	0.407 ± 0.124	0.588 ± 0.175	0.181	1.21×10^{-2}
ZNF385A	cg20967139	0.767 ± 0.059	0.685 ± 0.079	0.083	1.36×10^{-2}
ACSS1	cg23676480	0.750 ± 0.088	0.563 ± 0.247	0.187	1.49×10^{-2}
IL12RB1	cg06905726	0.754 ± 0.082	0.556 ± 0.273	0.199	1.53×10^{-2}

Note: All 124 probes designed for 104 genes showing significant correlations with either the largest tumor diameter or portal vein involvement are shown in Table S8, and the top 10 genes for each are summarized in this Table.

Abbreviation: HCC, hepatocellular carcinoma.

[a]Probe IDs for the Infinium HumanMethylation450 BeadChip (Illumina).

[b]Difference in β-values for the two groups.

mRNA expression of *PLEKHG2* was significantly elevated in U_{III}-T samples with portal vein involvement relative to U_{III}-T samples without it, along with DNA hypomethylation in U_{III}-T samples with portal vein involvement ($p = 6.04 \times 10^{-3}$ by Welch's *t*-test; Figure 5c).

DNA methylation status-related transcriptional regulation of cryptogenic HCC-related genes

Quantitative RT–PCR analysis showed the levels of *ADCY5* mRNA expression in the HCC cell lines (Figure 6a). The top two cell lines

showing the lowest levels of mRNA expression for *ADCY5* – HepG2 and JHH-7 – were subjected to Infinium assay and quantitative RT–PCR analysis after treatment with a demethylating agent – 5-aza-dC. Reduced DNA methylation levels and increased mRNA expression levels of *ADCY5* were confirmed in both HepG2 and JHH-7 (Figure 6b).

In the top two cell lines showing the lowest levels of mRNA expression for *MICAL2* (Figure 6c) – JHH-7 and HepG2 – reduced DNA methylation levels and increased mRNA expression levels of *MICAL2* were confirmed after 5-aza-dC treatment (Figure 6d). In the top two cell lines showing the lowest levels of mRNA expression for *PLEKHG2* (Figure 6e) – HepG2 and PLC/PRF5 – reduced DNA
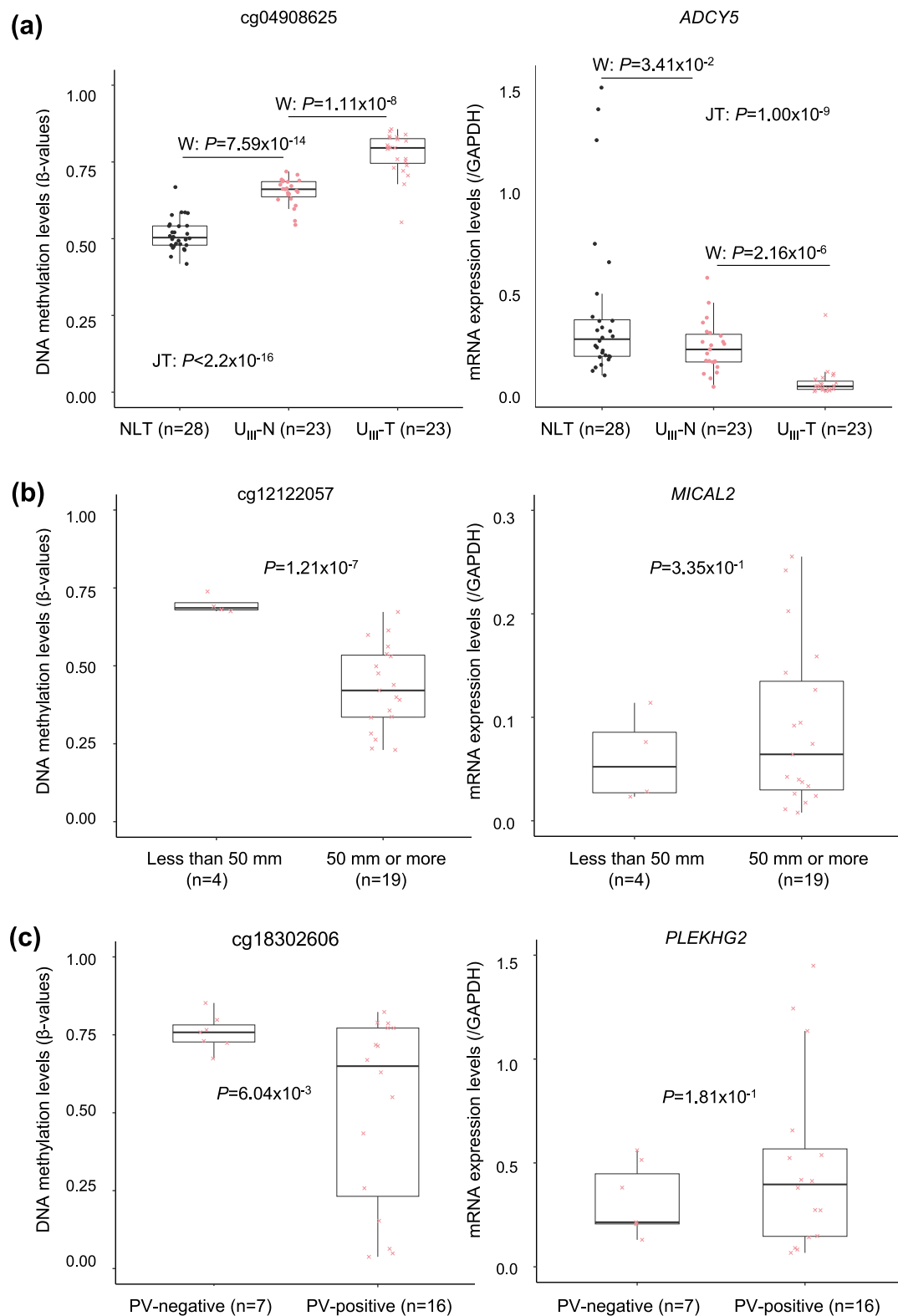
FIGURE 5 DNA methylation levels and mRNA expression levels for the *ADCY5*, *MICAL2*, and *PLEKHG2* genes. (a) Assays for *ADCY5* in samples of normal control liver tissue (NLT; $n = 28$), noncancerous liver tissue from patients with cryptogenic hepatocellular carcinoma (HCC) belonging to Cluster III (U_{III}-N) ($n = 23$) and the corresponding HCC (U_{III}-T) ($n = 23$). (b) Assays for *MICAL2* in U_{III}-Ts with a tumor diameter of less than 50 mm ($n = 4$) and U_{III}-Ts with a tumor diameter of 50 mm or more ($n = 19$). (c) Assays for *PLEKHG2* in U_{III}-Ts without ($n = 7$) and with ($n = 16$) portal vein involvement (PV). The Infinium probe ID is shown at the top of each panel. The p-values by Welch's t-test (W) and Jonckheere–Terpstra (JT) trend test are shown.
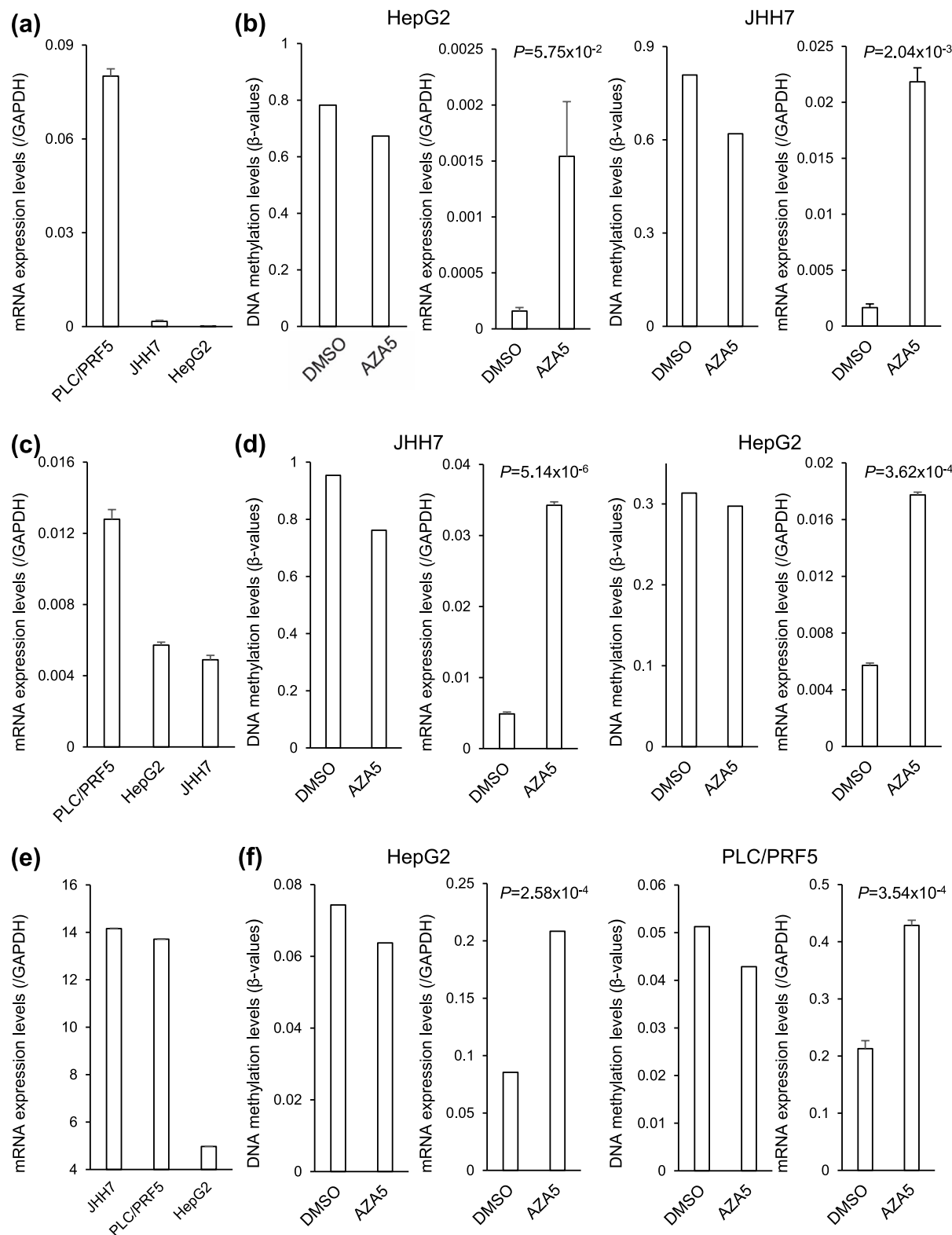
FIGURE 6 Treatment of hepatocellular carcinoma cell lines with 5-aza-2′-deoxycytidine (AZA5). (a) Quantitative reverse transcription polymerase chain reaction analysis of *ADCY5* mRNA expression. The top two cell lines showing the lowest levels of mRNA expression, HepG2 and JHH-7, were subjected to AZA5 treatment. (b) DNA methylation levels and mRNA expression levels of *ADCY5* in HepG2 and JHH-7 after AZA5 treatment. (c) Reverse transcription polymerase chain reaction of *MICAL2* mRNA expression. The top two cell lines showing the lowest levels of mRNA expression, JHH-7 and HepG2, were subjected to AZA5 treatment. (d) DNA methylation levels and mRNA expression levels of *MICAL2* in JHH-7 and HepG2 after AZA5 treatment. (e) Reverse transcription polymerase chain reaction analysis of *PLEKHG2* mRNA expression. The top two cell lines showing the lowest levels of mRNA expression, HepG2 and PLC/PRF5, were subjected to AZA5 treatment. (f) DNA methylation levels and mRNA expression levels of *PLEKHG2* in HepG2 and PLC/PRF5 after AZA5 treatment. DMSO, dimethylsulfoxide.

methylation levels and increased mRNA expression levels of *PLEKHG2* were confirmed after 5-aza-dC treatment (Figure 6f). In addition, as liver tissue consists of both parenchymal and nonparenchymal cells, the human immortalized hepatic stellate cell – TWNT-1[33] – and the human immortalized hepatic endothelial cell – TMNK-1[34] – were subjected to 5-aza-dC treatment (Figure S4). Although restoration of expression after 5-aza-dC treatment was not observed in TWNT-1 (data not shown), restoration of *ADCY5*, *MICAL2*, and *PLEKHG2* gene expression was confirmed in TMNK-1 (Figure S4), indicating that mRNA expression levels of the examined genes are regulated by DNA methylation status even in some nonparenchymal cells.

DISCUSSION

Principal component analysis clearly revealed that even U-N samples with no remarkable histological features showed a distinct DNA methylation profile differing from that of NLT samples, indicating that DNA methylation alterations have already occurred in apparently normal tissue at the precancerous stages, as is the case in the kidney[17–19] and urinary bladder.[20–22] DNA methylation alterations in U-N samples were inherited by or strengthened in U-T samples (Figure 3), just as our previous studies have shown that DNA methylation alterations in NASH-N[13–16] and V-N[4–9] samples are inherited by or strengthened in the corresponding HCCs. These findings indicate that U-N-specific DNA methylation alterations participate in cryptogenic hepatocarcinogenesis.

The 616 genes whose DNA methylation levels differed significantly between U_{III}-Ns and Other$_{I, II, IV}$-Ns, for which probes were designed on CpG islands, island shores, and island shelves around the transcription start site, and for which DNA methylation alterations could have potentially resulted in expression alterations based on The Cancer Genome Atlas database, were accumulated in molecular pathways involved in metabolic abnormalities (Table S7). There are two possible explanations for these findings: (1) metabolic abnormalities that are not reflected in the tissue histology occur in the precancerous stages of cryptogenic HCC with unknown etiology; or (2) NASH-N specimens account for a large proportion of Other$_{I, II, and IV}$-Ns, and the results of pathway analysis reflect the fact that NASH is a metabolic disorder.[10]

The *ADCY5* gene was the only gene to show U_{III}-N-specific DNA methylation abnormalities when compared with NLT samples. DNA hypermethylation of *ADCY5* is specifically associated with the development of U-Ts even from the precancerous U-N stage. Moreover, our treatment with demethylating agents indicated that *ADCY5* expression is regulated by DNA methylation levels in human HCC cells. *ADCY5* is a member of the membrane-bound adenylate cyclase family, and is responsible for the conversion of adenosine triphosphate to cyclic adenosine-3′, 5′-monophosphate. Cyclic adenosine-3′, 5′-monophosphate is a second messenger that exerts a wide variety of effects through several signaling pathways (Table S9).[35] Moreover, we and other groups have reported DNA hypermethylation and reduced

expression of *ADCY5* in lung cancer[36] and lymphocytic leukemia.[37] In liver-specific COX-2 transgenic mice, DNA hypermethylation and reduced expression of *ADCY5* were observed in spontaneously developed HCCs,[38] indicating that *ADCY5* has tumor-suppressive effects in the liver. As HCCs in COX-2 transgenic mice had inflammation in their background liver,[38] it remains to be clarified further whether human cryptogenic hepatocarcinogenesis is associated with "ultra-microinflammation," even though microscopy revealed no obvious inflammatory cell infiltration in U-N samples.

Among the eight genes other than *ADCY5* in Table 2, *RAB3D*, a RAS oncogene family member, shows DNA hypomethylation in U_{III}-N samples, potentially resulting in upregulation during the developmental stage of U_{III}-T. This is consistent with a previous report that *RAB3D* is upregulated in HCC cells and enhances the malignant phenotype of HCCs through the Warburg effect.[39] A transcription factor, *ZNF385A*, showed DNA hypomethylation in U_{III}-N samples, and may be upregulated during U_{III}-T development, which is consistent with a previous report that overexpression of *ZNF385A* in HCCs is associated with poorer prognosis.[40] *ARHGEF2*, a Rho/Rac guanine nucleotide exchange factor, again shows DNA hypomethylation in U_{III}-N samples, which is consistent with a previous report that *ARHGEF2* overexpression is associated with malignant progression of HCCs.[41] In contrast, *HADH* involved in fatty acid β-oxidation showed DNA hypermethylation in U_{III}-N samples. This is consistent with a previous study indicating that *HADH* expression is decreased in cultured HCC cells.[42] Taken together, it has been confirmed that the present analysis efficiently identified the genes involved in hepatocarcinogenesis.

The top two genes for which DNA hypomethylation in U-T samples significantly correlated with the largest tumor diameter and portal vein involvement were *MICAL2* and *PLEKHG2*, respectively. MICAL family members are associated with cytoskeletal remodeling and cell migration (Table S9),[43] which can result in invasion and metastasis.[44] *MICAL2* is reportedly overexpressed in various tumors, including gastric cancer[45] and lung cancer.[46] Moreover, silencing of *MICAL2* promotes mesenchymal to epithelial transition, and inhibits the viability, as well as the motility and invasive properties, of human cancer cells.[47] Therefore, it is feasible that DNA hypomethylation of *MICAL2* would play a role in the determination of the clinicopathological feature of U-Ts through its overexpression. In addition, it has been reported that overexpression of *MICAL2* is involved in inflammation-induced angiogenesis in animal models.[48] Therefore, even though microscopy revealed no obvious inflammatory cell infiltration in U-N samples, "ultra-microinflammation" may affect the clinicopathological feature of cryptogenic HCC through DNA hypomethylation of *MICAL2*.

PLEKHG2 is a G-protein-coupled receptor-related gene.[49] The Reactome database has shown that *PLEKHG2* participates in several signaling pathways related to cell death, proliferation, and migration (Table S9). Although the correlation between *PLEKHG2* and HCCs and abnormal DNA methylation of *PLEKHG2* in cancers have not yet been reported, overexpression of *PLEKHG2* mRNA is reportedly associated with a poorer outcome in patients with lung

adenocarcinoma, pediatric brain tumor, and breast cancer.[50] Therefore, it is again feasible that DNA hypomethylation of *PLEKHG2* might determine the clinicopathological feature of cryptogenic HCCs through overexpression of *PLEKHG2*.

In summary, the Infinium assay has shown the presence of U-N-specific DNA methylation profiles in liver tissue samples, including DNA hypermethylation of the *ADCY5* gene, and indicated that DNA methylation alterations participate in cryptogenic hepatocarcinogenesis even from the early and precancerous U-N stage. Clinicopathological features of U-Ts may be determined by DNA methylation alterations of specific tumor-related genes, such as *MICAL2* and *PLEKHG2* in tumorous tissue. Genome-wide DNA methylation analysis will be a powerful tool for revealing the molecular backgrounds of cryptogenic HCCs.

CONFLICT OF INTEREST STATEMENT

Authors declare no Conflict of Interests for this article.

DATA AVAILABILITY STATEMENT

The results of the Infinium assay have been deposited in the Gene Expression Omnibus (GEO) database (https://www.ncbi.nlm.nih.gov/geo/; accession numbers: GSE89852, GSE183468, and GSE233160).

ETHICS STATEMENT

Approval of the research protocol: This study was approved by the Ethics Committees of Keio University School of Medicine and the National Cancer Center, Tokyo, Japan.

Informed Consent: All patients gave written informed consent for inclusion of their specimens in this study.

Registry and the Registration No. of the study/trial: N/A.

Animal Studies: N/A.

Research involving recombinant DNA: N/A.

ORCID

Mao Fujimoto ⓘ https://orcid.org/0000-0002-2020-935X

Yae Kanai ⓘ https://orcid.org/0000-0002-7904-9506

Eri Arai ⓘ https://orcid.org/0000-0002-0076-4823

REFERENCES

1. Kim M, Delgado E, Ko S. DNA methylation in cell plasticity and malignant transformation in liver diseases. Pharmacol Ther. 2023; 241:108334. https://doi.org/10.1016/j.pharmthera.2022.108334
2. Jones PA, Issa JP, Baylin S. Targeting the cancer epigenome for therapy. Nat Rev Genet. 2016;17(10):630–41. https://doi.org/10.1038/nrg.2016.93
3. Baylin SB, Jones PA. Epigenetic determinants of cancer. Cold Spring Harbor Perspect Biol. 2016;8(9):a019505. https://doi.org/10.1101/cshperspect.a019505
4. Nagashio R, Arai E, Ojima H, Kosuge T, Kondo Y, Kanai Y. Carcinogenetic risk estimation based on quantification of DNA methylation levels in liver tissue at the precancerous stage. Int J Cancer. 2011; 129(5):1170–9. https://doi.org/10.1002/ijc.26061
5. Arai E, Ushijima S, Gotoh M, Ojima H, Kosuge T, Hosoda F, et al. Genome-wide DNA methylation profiles in liver tissue at the precancerous stage and in hepatocellular carcinoma. Int J Cancer. 2009; 125(12):2854–62. https://doi.org/10.1002/ijc.24708
6. Saito Y, Kanai Y, Sakamoto M, Saito H, Ishii H, Hirohashi S. Overexpression of a splice variant of DNA methyltransferase 3b, DNMT3b4, associated with DNA hypomethylation on pericentromeric satellite regions during human hepatocarcinogenesis. Proc Natl Acad Sci USA. 2002;99(15):10060–5. https://doi.org/10.1073/pnas.152121799
7. Yamamoto H, Itoh F, Fukushima H, Kaneto H, Sasaki S, Ohmura T, et al. Infrequent widespread microsatellite instability in hepatocellular carcinomas. Int J Oncol. 2000;16:543–7. https://doi.org/10.3892/ijo.16.3.543
8. Kondo Y, Kanai Y, Sakamoto M, Mizokami M, Ueda R, Hirohashi S. Genetic instability and aberrant DNA methylation in chronic hepatitis and cirrhosis--A comprehensive study of loss of heterozygosity and microsatellite instability at 39 loci and DNA hypermethylation on 8 CpG islands in microdissected specimens from patients with hepatocellular carcinoma. Hepatology. 2000;32(5):970–9. https://doi.org/10.1053/jhep.2000.19797
9. Kanai Y, Ushijima S, Tsuda H, Sakamoto M, Sugimura T, Hirohashi S. Aberrant DNA methylation on chromosome 16 is an early event in hepatocarcinogenesis. Jpn J Cancer Res. 1996;87(12):1210–7. https://doi.org/10.1111/j.1349-7006.1996.tb03135.x
10. Powell EE, Wong VW, Rinella M. Non-alcoholic fatty liver disease. Lancet. 2021;397(10290):2212–24. https://doi.org/10.1016/s0140-6736(20)32511-3
11. Marengo A, Rosso C, Bugianesi E. Liver cancer: connections with obesity, fatty liver, and cirrhosis. Annu Rev Med. 2016;67(1): 103–17. https://doi.org/10.1146/annurev-med-090514-013832
12. Bibikova M, Le J, Barnes B, Saedinia-Melnyk S, Zhou L, Shen R, et al. Genome-wide DNA methylation profiling using Infinium® assay. Epigenomics. 2009;1:177–200. https://doi.org/10.2217/epi.09.14
13. Kuramoto J, Arai E, Fujimoto M, Tian Y, Yamada Y, Yotani T, et al. Quantification of DNA methylation for carcinogenic risk estimation in patients with non-alcoholic steatohepatitis. Clin Epigenet. 2022; 14(1):168. https://doi.org/10.1186/s13148-022-01379-4
14. Kuramoto J, Arai E, Tian Y, Funahashi N, Hiramoto M, Nammo T, et al. Genome-wide DNA methylation analysis during non-alcoholic steatohepatitis-related multistage hepatocarcinogenesis: comparison with hepatitis virus-related carcinogenesis. Carcinogenesis. 2017;38(3):261–70. https://doi.org/10.1093/carcin/bgx005
15. Tsuda N, Tian Y, Fujimoto M, Kuramoto J, Makiuchi S, Ojima H, et al. DNA methylation status of the SPHK1 and LTB genes underlies the clinicopathological diversity of non-alcoholic steatohepatitis-related hepatocellular carcinomas. J Cancer Res Clin Oncol. 2022;149(8): 5109–25. https://doi.org/10.1007/s00432-022-04445-9
16. Tian Y, Arai E, Makiuchi S, Tsuda N, Kuramoto J, Ohara K, et al. Aberrant DNA methylation results in altered gene expression in non-alcoholic steatohepatitis-related hepatocellular carcinomas. J Cancer Res Clin Oncol. 2020;146(10):2461–77. https://doi.org/10.1007/s00432-020-03298-4
17. Arai E, Chiku S, Mori T, Gotoh M, Nakagawa T, Fujimoto H, et al. Single-CpG-resolution methylome analysis identifies clinicopathologically aggressive CpG island methylator phenotype clear cell renal cell carcinomas. Carcinogenesis. 2012;33(8):1487–93. https://doi.org/10.1093/carcin/bgs177
18. Arai E, Ushijima S, Fujimoto H, Hosoda F, Shibata T, Kondo T, et al. Genome-wide DNA methylation profiles in both precancerous

conditions and clear cell renal cell carcinomas are correlated with malignant potential and patient outcome. Carcinogenesis. 2009;30(2):214–21. https://doi.org/10.1093/carcin/bgn268

19. Arai E, Kanai Y, Ushijima S, Fujimoto H, Mukai K, Hirohashi S. Regional DNA hypermethylation and DNA methyltransferase (DNMT) 1 protein overexpression in both renal tumors and corresponding nontumorous renal tissues. Int J Cancer. 2006;119(2):288–96. https://doi.org/10.1002/ijc.21807

20. Tsumura K, Arai E, Tian Y, Shibuya A, Nishihara H, Yotani T, et al. Establishment of permutation for cancer risk estimation in the urothelium based on genome-wide DNA methylation analysis. Carcinogenesis. 2019;40(11):1308–19. https://doi.org/10.1093/carcin/bgz112

21. Nishiyama N, Arai E, Chihara Y, Fujimoto H, Hosoda F, Shibata T, et al. Genome-wide DNA methylation profiles in urothelial carcinomas and urothelia at the precancerous stage. Cancer Sci. 2010;101(1):231–40. https://doi.org/10.1111/j.1349-7006.2009.01330.x

22. Nakagawa T, Kanai Y, Saito Y, Kitamura T, Kakizoe T, Hirohashi S. Increased DNA methyltransferase 1 protein expression in human transitional cell carcinoma of the bladder. J Urol. 2003;170:2463–6. https://doi.org/10.1097/01.ju.0000095919.50869.c9

23. de Mattos ÂZ, Debes JD, Boonstra A, Yang JD, Balderramo DC, Sartori GDP, et al. Current impact of viral hepatitis on liver cancer development: the challenge remains. World J Gastroenterol. 2021;27(24):3556–67. https://doi.org/10.3748/wjg.v27.i24.3556

24. Seitz HK, Bataller R, Cortez-Pinto H, Gao B, Gual A, Lackner C, et al. Alcoholic liver disease. Nat Rev Dis Prim. 2018;4(1):16. https://doi.org/10.1038/s41572-018-0014-7

25. Brunt EM, Kleiner DE, Wilson LA. Belt P, Neuschwander-Tetri BA, NASH Clinical Research Network (CRN). Nonalcoholic fatty liver disease (NAFLD) activity score and the histopathologic diagnosis in NAFLD: distinct clinicopathologic meanings. Hepatology. 2011;53(3):810–20. https://doi.org/10.1002/hep.24127

26. Torbenson MS, Ng IOL, Park YN, Roncali M, Sakamoto M. Hepatocellular carcinoma. In: World Health Organization classification of tumours Digestive system tumors. 5th ed, 1. Lyon: IARC Press; 2019. p. 229–39.

27. Kanai Y, Nishihara H, Miyagi Y, Tsuruyama T, Taguchi K, Katoh H, et al. The Japanese Society of Pathology Guidelines on the handling of pathological tissue samples for genomic research: standard operating procedures based on empirical analyses. Pathol Int. 2018;68(2):63–90. https://doi.org/10.1111/pin.12631

28. MacNab GM, Alexander JJ, Lecatsas G, Bey EM, Urbanowicz JM. Hepatitis B surface antigen produced by a human hepatoma cell line. Br J Cancer. 2017;34(5):509–15. https://doi.org/10.1038/bjc.1976.205

29. Fujise K, Nagamori S, Hasumura S, et al. Integration of hepatitis B virus DNA into cells of six established human hepatocellular carcinoma cell lines. Hepato-Gastroenterology. 1990;37:457–60.

30. Dor I, Namba M, Sato J. Establishment and some biological characteristics of human hepatoma cell lines. Gan. 1975;66:385–92.

31. Hirano T, Arai E, Fujimoto M, Nakayama Y, Tian Y, Ito N, et al. Prognostication of early-onset endometrioid endometrial cancer based on genome-wide DNA methylation profiles. J Gynecol Oncol. 2022;33(6):e74. https://doi.org/10.3802/jgo.2022.33.e74

32. Fujimoto M, Arai E, Tsumura K, Yotani T, Yamada Y, Takahashi Y, et al. Establishment of diagnostic criteria for upper urinary tract urothelial carcinoma based on genome-wide DNA methylation analysis. Epigenetics. 2020;15(12):1289–301. https://doi.org/10.1080/15592294.2020.1767374

33. Watanabe T, Shibata N, Westerman KA, Okitsu T, Allain JE, Sakaguchi M, et al. Establishment of immortalized human hepatic stellate scavenger cells to develop bioartificial livers. Transplantation.

2003;75(11):1873–80. https://doi.org/10.1097/01.tp.0000064621.50907.a6

34. Matsumura T, Takesue M, Westerman KA, Okitsu T, Sakaguchi M, Fukazawa T, et al. Establishment of an immortalized human-liver endothelial cell line with SV40T and hTERT. Transplantation. 2004;77(9):1357–65. https://doi.org/10.1097/01.tp.0000124286.82961.7e

35. Doyle TB, Hayes MP, Chen DH, Raskind WH, Watts VJ. Functional characterization of AC5 gain-of-function variants: impact on the molecular basis of ADCY5-related dyskinesia. Biochem Pharmacol. 2019;163:169–77. https://doi.org/10.1016/j.bcp.2019.02.005

36. Sato T, Arai E, Kohno T, Tsuta K, Watanabe S, Soejima K, et al. DNA methylation profiles at precancerous stages associated with recurrence of lung adenocarcinoma. PLoS One. 2013;8(3):e59444. https://doi.org/10.1371/journal.pone.0059444

37. Tong WG, Wierda WG, Lin E, Kuang SQ, Bekele BN, Estrov Z, et al. Genome-wide DNA methylation profiling of chronic lymphocytic leukemia allows identification of epigenetically repressed molecular pathways with clinical impact. Epigenetics. 2010;5(6):499–508. https://doi.org/10.4161/epi.5.6.12179

38. Chen H, Cai W, Chu ESH, Tang J, Wong CC, Wong SH, et al. Hepatic cyclooxygenase-2 overexpression induced spontaneous hepatocellular carcinoma formation in mice. Oncogene. 2017;36(31):4415–26. https://doi.org/10.1038/onc.2017.73

39. Li S, Liu Y, Bai Y, Chen M, Cheng D, Wu M, et al. Ras homolog family member F, filopodia associated promotes hepatocellular carcinoma metastasis by altering the metabolic status of cancer cells through RAB3D. Hepatology. 2021;73(6):2361–79. https://doi.org/10.1002/hep.31641

40. Peng Q, Li J, Wu Q, Wang P, Kang Z, Deng Y, et al. ZNF385A and ZNF346 serve as prognostic biomarkers associated with an inflamed immunosuppressive tumor microenvironment in hepatocellular carcinoma. Int J Mol Sci. 2023;24(4):3155. https://doi.org/10.3390/ijms24043155

41. Zhu Y, Liu W, Wang Z, Wang Y, Pan Z, et al. ARHGEF2/EDN1 pathway participates in ER stress-related drug resistance of hepatocellular carcinoma by promoting angiogenesis and malignant proliferation. Cell Death Dis. 2022;13(7):652. https://doi.org/10.1038/s41419-022-05099-8

42. Nwosu ZC, Battello N, Rothley M, Piorońska W, Sitek B, Ebert MP, et al. Liver cancer cell lines distinctly mimic the metabolic gene expression pattern of the corresponding human tumours. J Exp Clin Cancer Res. 2018;37(1):211. https://doi.org/10.1186/s13046-018-0872-6

43. Rajan S, Terman JR, Reisler E. MICAL-mediated oxidation of actin and its effects on cytoskeletal and cellular dynamics. Front Cell Dev Biol. 2023;11:1124202. https://doi.org/10.3389/fcell.2023.1124202

44. Aseervatham J. Cytoskeletal remodeling in cancer. Biology. 2020;9(11):385. https://doi.org/10.3390/biology9110385

45. Wang Q, Qi C, Min P, Wang Y, Ye F, Xia T, et al. MICAL2 contributes to gastric cancer cell migration via Cdc42-dependent activation of E-cadherin/β-catenin signaling pathway. Cell Commun Signal. 2022;20(1):136. https://doi.org/10.1186/s12964-022-00952-x

46. Zhou W, Liu Y, Gao Y, Cheng Y, Chang R, Li X, et al. MICAL2 is a novel nucleocytoplasmic shuttling protein promoting cancer invasion and growth of lung adenocarcinoma. Cancer Lett. 2020;483:75–86. https://doi.org/10.1016/j.canlet.2020.04.019

47. Mariotti S, Barravecchia I, Vindigni C, Pucci A, Balsamo M, Libro R, et al. MICAL2 is a novel human cancer gene controlling mesenchymal to epithelial transition involved in cancer growth and invasion. Oncotarget. 2016;7(2):1808–25. https://doi.org/10.18632/oncotarget.6577

48. Barravecchia I, Mariotti S, Pucci A, Scebba F, De Cesari C, Bicciato S, et al. MICAL2 is expressed in cancer associated neo-angiogenic capillary endothelia and it is required for endothelial cell viability, motility and VEGF response. Biochim Biophys Acta, Mol Basis Dis. 2019;1865(9):2111–24. https://doi.org/10.1016/j.bbadis.2019.04.008

49. Sugiyama K, Tago K, Matsushita S, Nishikawa M, Sato K, Muto Y, et al. Heterotrimeric G protein Gαs subunit attenuates PLEKHG2, a Rho family-specific guanine nucleotide exchange factor, by direct interaction. Cell Signal. 2017;32:115–23. https://doi.org/10.1016/j.cellsig.2017.01.022

50. Zhang Y, Chen F, Pleasance E, Williamson L, Grisdale CJ, Titmuss E, et al. Rearrangement-mediated cis-regulatory alterations in advanced patient tumors reveal interactions with therapy. Cell Rep. 2021;37(7):110023. https://doi.org/10.1016/j.celrep.2021.110023

SUPPORTING INFORMATION

Additional supporting information can be found online in the Supporting Information section at the end of this article.